Agricultural and Forest Meteorology 164 (2012) 136–148

Contents lists available at SciVerse ScienceDirect

Agricultural and Forest Meteorology

journal homepage: www.elsevier.com/locate/agrformet

Effects of water availability on carbon and water exchange in a young ponderosa pine forest: Above- and belowground responses

Nadine K. Ruehr[a,b,*], Jonathan G. Martin[a], Beverly E. Law[a]

[a] Oregon State University, College of Forestry, Department of Forest Ecosystems & Society, Corvallis, OR 97331, USA
[b] Karlsruhe Institute of Technology (KIT), Institute of Meteorology and Climate Research – Atmospheric Environmental Research, 82467 Garmisch-Partenkirchen, Germany

ARTICLE INFO

Article history:
Received 22 July 2011
Received in revised form 11 April 2012
Accepted 22 May 2012

Keywords:
Drought
Irrigation
Transpiration
Stomatal conductance
Photosynthesis
Soil respiration

ABSTRACT

Changes in the hydrological cycle, as predicted and currently observed, are expected to significantly impact the water and carbon balance of water-limited forest ecosystems. However, differences in the water-sensitivity of component processes make carbon balance predictions challenging. To examine responses of ecosystem components to water limitations, we conducted a study of tree, soil and ecosystem-level processes in a young ponderosa pine stand under natural summer drought (control) and increased soil water conditions (watered). Weekly-averaged tree transpiration (T_{tree}), gross ecosystem photosynthesis (GPP) and soil CO_2 efflux (Rs_{tree}; nearby trees) were related with soil water content (SWC; polynomial form: T_{tree} R^2 = 0.98 and Rs_{tree} R^2 = 0.91, logarithmic form: GPP R^2 = 0.86) and declined rapidly when relative extractable soil water (REW) was <50%. The sensitivity of daily variations in canopy conductance (G_s) to vapor pressure deficit was affected by SWC (R^2 = 0.97; logarithmic function), decreasing at REW <50%. Watering maintained REW at about 70% in July and August but positively affected tree carbon and water dynamics only at the end of summer when fluxes in the control treatment were strongly water-limited. A tight coupling of above- and belowground fluxes became apparent. In the control treatment, root-rhizosphere respiration (Rr) decreased along with GPP and T_{tree} (R^2 = 0.58) as drought progressed, while watering maintained Rr, T_{tree} and G_s at a significantly higher level than those of the unwatered trees in late summer. In contrast, microbial respiration responded instantaneously and strongly to the watering compared to the control treatment. The net effect was that increased soil water availability during the typical dry growing season has a negative effect on the short-term seasonal ecosystem C balance due to a larger increase in decomposition than photosynthesis. However, longer-term effects remain uncertain. In summary, our study highlights that understanding the dissimilar response of tree dynamics and soil decomposition to water availability is a key component in predicting future C sequestration in water-limited forest ecosystems.

1. Introduction

Net ecosystem productivity (NEP) is the delicate balance between photosynthesis (C gain) and respiration (C loss) processes that are tightly coupled to the water cycle. Under water-stress conditions (atmospheric and soil water deficit), transpiration is controlled by stomatal conductance to prevent loss of function of the hydraulic system while minimizing limitations to carbon uptake (Meinzer, 2002; Chaves et al., 2003). While leaf and root respiration mostly decreases along with photosynthesis in response to drought (for a detailed review see Atkin and Macherel, 2009), microbial respiration has often been found to be less sensitive, probably due to increasing temperatures partially compensating for soil moisture constrains on decomposition (e.g., Lavigne et al., 2004; Irvine et al., 2008). Thus, the magnitude and direction of how drought severity affects NEP depends on the water-sensitivity as well as degree of water-limitation of each of the processes involved. For instance, under modest drought stress, when trees have access to deep soil water while the surface is dry, microbial respiration might be more limited than photosynthesis, thus the net C uptake would remain positive (e.g., Reichstein et al., 2002; Thomas et al., 2009). However, under more severe drought, photosynthesis has been found to generally decrease more strongly than respiration (Schwalm et al., 2009), so that ecosystems might become a CO_2 source to the atmosphere (Granier et al., 2007; Pereira et al., 2007). Thus, a detailed understanding of ecosystem process dynamics to variations in water availability is critical to enhance predictions of ecosystems' C sink strength under future conditions (Reichstein et al., 2007; Jentsch and Beierkuhnlein, 2008; Gerten et al., 2008; Ryan, 2011). Most of the information available on

* Corresponding author.
E-mail address: nadine.ruehr@kit.edu (N.K. Ruehr).

0168-1923/$ – see front matter © 2012 Elsevier B.V. All rights reserved.
http://dx.doi.org/10.1016/j.agrformet.2012.05.015

responses of forest ecosystems to changes in water availability is from field observations during occasional and seasonal dry spells. Some studies manipulate water availability in forests (either by throughfall reduction or irrigation) allowing examination of the fundamental control of soil water availability on ecosystem processes. Often these studies focus either on short-term plant (e.g., Panek and Goldstein, 2001) or more longterm soil processes (e.g., Froberg et al., 2008), but less information is available on concurrent responses of processes in the plant–soil-system and net effects from photosynthesis and respiration.

Semi-arid and Mediterranean type forest ecosystems are going to be strongly affected by alterations in water availability as predicted with climate change (Schroter et al., 2005; Gerten et al., 2008). This is not surprising, as water availability is the main driver of the ecosystem carbon balance in these forest ecosystems (e.g., Pereira et al., 2007; Thomas et al., 2009). Ponderosa pine (*Pinus ponderosa* Dougl. ex Laws.) forests cover wide areas in semi-arid to Mediterranean climate zones of the United States. Recently, stand-replacing fires in western US *P. ponderosa* have been increasing due to higher stand densities and warmer temperatures, and are expected to further intensify in a more drought-prone future (Pierce et al., 2004). This may cause a shift in forest age-structures towards younger (planted or natural regenerated) ponderosa pine stands, and subsequently amplify the sensitivity of this forest type to future conditions, as young trees are generally found to be more vulnerable to drought conditions (Hanson and Weltzin, 2000). Indeed, studies in young ponderosa pine reveal its high sensitivity to changes in precipitation patterns and drought severity (Goldstein et al., 2000; Irvine et al., 2002, 2004). Several mechanisms may come into play. Domec et al. (2004) found the hydraulic system in young compared to mature trees to be more vulnerable to root embolisms that can act in phase with stomata to limit water loss and thus C uptake. Moreover, young trees appear to use water reserves less conservatively than old stands (Irvine et al., 2002, 2004), have reduced access to water deeper in the soil column due to shallower rooting (Williams et al., 2001; Brooks et al., 2002) and show high vulnerability to extreme heat events that may lead to cavitation in the water conducting system and significantly impact NEE (Goldstein et al., 2000). Thus, changes in water availability as suggested by climate predictions for this region (e.g., wetter winter/spring and drier summer), can be expected to strongly affect the carbon and water balance of these semi-arid, regenerating forest stands.

In this study, we investigated the degree of coupling of CO_2 and H_2O fluxes and examined their dependence on soil water content (SWC) and atmospheric water deficit (VPD) at the ecosystem, tree and soil level in a post-fire regenerating young ponderosa pine stand. We closely followed CO_2 and H_2O flux dynamics during the summer dry season, and compared flux dynamics to a well watered treatment. We hypothesized (1) tree carbon and water fluxes are tightly coupled, (2) root respiration is in-phase with aboveground flux dynamics (in contrast to microbial respiration), and (3) photosynthesis increases relatively more than respiration along with increasing water availability.

2. Methods

2.1. Study site

The study site (US-Me6) is located east of the Cascade Mountains, near Sisters, Central Oregon (977 m a.s.l., 44°19′25.5″N, −121°36′18.4″E) and is part of the Metolius cluster sites with different age and disturbance classes within the AmeriFlux network. After a severe fire in 1979, the site was salvage logged, became US Forest Service land and was largely re-forested in 1986.

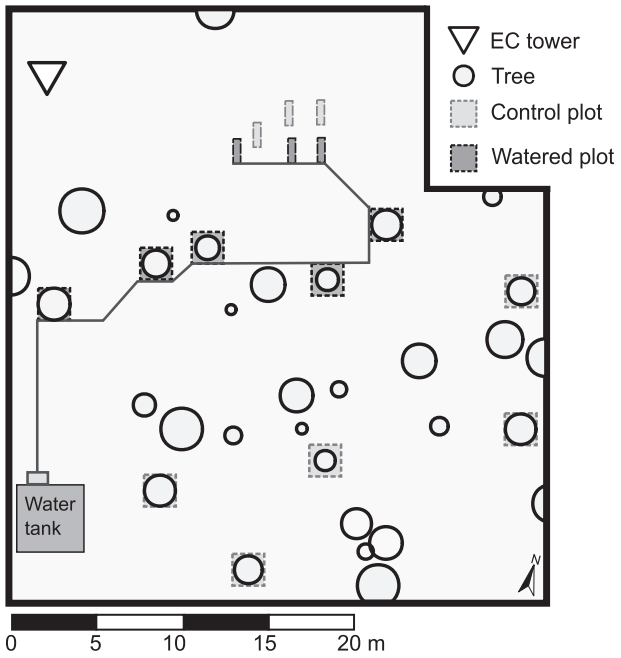

Fig. 1. Map of the experimental set-up at the young ponderosa pine study site in Central Oregon (US-Me6). The location of trees, the plots of the control and watered treatment, as well as the set-up of the irrigation system are shown.

Due to poor survival additional planting was conducted in 1990. The dominant overstory vegetation is 22–26-year old *P. ponderosa* with an average height of 5.2 ±1.1 m. Summer maximum half-sided leaf area index (LAI) was 0.8 m^2 m^{-2} in 2010. Tree density is low with 162 trees ha^{-1}. The understory vegetation is scattered and dominated by antelope bitterbrush (*Purshia tridentata* (Pursh) D.C.) and grasses (predominantly *Bromus tectorum* L.), with few ponderosa pine saplings and greenleaf manzanitas (*Arctostaphylos patula* Greene) interspersed. The soil is a freely draining sandy loam (80% sand, 20% silt), derived from volcanic ash (soil depth > 1 m). The climate can be described as Mediterranean with hot, dry summers and cool, wet springs and winters with precipitation mainly falling as rain and occasionally snow when the site is in the polar front region. The longterm 30-year (1971–2000) precipitation average is 460 mm with average monthly minimum and maximum temperatures ranging between −5.5 and 10.5 during winter, and 2.5 and 27.8 °C during summer (PRISM Climate Group, Oregon State University, http://prism.oregonstate.edu, created 31 Oct 2008).

2.2. Experimental setup

About 50 m southeast of a flux tower within an area of about 30 × 30 m, 10 trees were selected and assigned to the control and watered treatment (Fig. 1). To ensure representativeness of the trees within the tower footprint and to ensure a relatively homogenous sample, we choose trees with similar height (control: 4.17 ± 0.27 m, watered: 3.94 ± 0.26 m), lush green needles and healthy appearance. Selected trees were more than 3 m apart from each other, and treated as independent plots. An area of 2 × 2 m surrounding each tree was assigned to soil CO_2 efflux, soil temperature and moisture measurements that generally represented the area under the crown and largely horizontal root distribution (Law et al., 2001a).

To partition soil CO_2 efflux under trees (Rs_{tree}) into root and microbial respiration, we measured soil CO_2 efflux on plots in existing gaps within the forest (0.5 × 1.5 m, n = 3 per treatment), where the measurements were at least 5 m away from the nearest tree (Fig. 1). Soil CO_2 efflux from these plots reflects mostly

microbial respiration (Rm; e.g., see Brumme, 1995; Tang et al., 2005), as plots were kept free of herbaceous and grassy ground vegetation (which are mainly dormant from about mid July onwards) and root invasion was negligible. Root coring at the end of the experiment to 30 cm depth resulted in 8 g m^{-2} woody fine roots and 33 g m^{-2} herbaceous/grassy fine roots (compare to 420 g m^{-2} fine root biomass in the tree plots).

Soil moisture (10HS, Decagon Devices, Inc., WA, USA) and temperature probes (Hobo Pro Series, Onset Computer Corporation, Bourne, MA, USA) were installed at 10 cm depth in each plot. To monitor deeper soil water content (SWC) we inserted additional soil moisture probes at 30 cm depth ($n = 2$, per treatment). To increase accuracy of SWC measurements, we calibrated the 10HS sensors to the site-specific soil to produce estimates of absolute SWC ($\pm 0.02\ m^3 m^{-3}$). The difference in SWC (10 cm depth) between the plots in the open and under the trees in both treatments was minor and within the range of accuracy of the SWC probes ($<0.02\ m^3 m^{-3}$), thus we provide SWC for the tree plots only. Relative extractable soil water (REW) was calculated as the ratio of actual extractable water to maximum extractable water following Granier et al. (2000). Minimum SWC was estimated as $0.06\ m^3 m^{-3}$ with a water retention curve (using data from a young ponderosa pine stand close-by; Irvine et al. (2002)). Maximum water content was approximated as the SWC after 1 day of drainage after the wettest SWC had been reached ($0.24\ m^3\ m^{-3}$). REW was calculated for the single soil depth of 30 cm, as this is about the average depth from which the majority of water extraction in young ponderosa pine is occurring (Irvine et al., 2004).

Plots assigned to the watered treatment were equipped with pressure-regulated drippers (Dig Irrigation Products, Vista, CA, USA). To ensure homogenous distribution of irrigation water, drippers were spaced uniformly so that each dripper covered an area of 0.25 m^2. Irrigation timing and amount was controlled by a timer connected to a water pump. Constant pressure ensured uniform water supply with only a small variation of ±5% between drippers. Irrigation was started after the last rain event on 24 June 2010, when SWC was high. Plots were supplied with water every other day, averaging at 5.5 mm d^{-1} (i.e., 22 l d^{-1} per tree) between 24 June and 23 July, and 7.3 mm d^{-1} (i.e., 29 l d^{-1} per tree) between 24 July and 31 August. The amount of supplied water was largely sufficient to maintain transpiration, since tree water-use under non-water limiting summer conditions averaged 26 l d^{-1} in July. In total, we applied about 9720 l of water (approx. 1700 l per tree) to the watered treatment between 24 June and 31 August 2010.

2.3. Flux tower and meteorological data

Meteorological parameters included air temperature (T_a; HMP45C, Vaisala, Helsinki, Finland and RTD-1000, R.M. Young Company, Traverse City, MI, USA) and relative humidity (RH; HMP45C, Vaisala, Helsinki, Finland), photosynthetic active radiation (PAR; PARlite, Kipp & Zonen, Delft, The Netherlands) and precipitation (TE525MM with 8″ funnel, Campbell Scientific, Logan, UT) that were measured at about 14 m aboveground. Ecosystem evapotranspiration and carbon exchange were estimated by the eddy-covariance (EC) technique. In brief, the EC measurement setup consisted of a three-dimensional sonic anemometer (CSAT3, Campbell Scientific, Logan, UT, USA) and an open path infrared gas analyzer (Li-7500, Li-Cor, Lincoln, NB, USA) deployed 14 m aboveground. We applied initial quality control and eddy-covariance flux calculations to compute 30-min averages as described in Thomas et al. (2009). Data during rain as well as extraordinary high fluxes (>20 μmol CO_2 m^{-2} s^{-1}) were discarded (only 2% of the data).

2.4. Transpiration and canopy conductance

We measured sap flux density of each tree using the heat dissipation technique (Granier, 1987), as described for *P. ponderosa* in more detail by Irvine et al. (2002). In brief, sap velocities were calculated from probe temperature differentials based on an empirical relationship (Granier, 1987). Zero flow was estimate from nights when VPD ≤ 0.3 kPa and linearly interpolated between nights. All xylem was assumed to transport water, as young ponderosa pine trees have not developed heartwood yet (Irvine et al., 2002). To scale sap flux to ground area we multiplied sap velocities and sapwood area. Sapwood area was derived from tree inventories of 4 × 17 m radius plots by estimating diameter at sensor height (30 cm below first branches) from diameter at breast height using a tapering equation ($y = 1.11x + 1.18$, $R^2 = 0.95$) and subtracting average bark thickness (0.7 cm). We also accounted for the decrease of sap flux density with sapwood depth as published in Irvine et al. (2004). Small data gaps (≤1 h) were linearly interpolated. Unfortunately, due to failure of two sensors, sap flux data were only available for four trees per treatment. To derive estimates of transpiration (T_{tree}) from sap flux, one has to account for the time lag between water uptake and transpiration caused by stem water storage (Schulze et al., 1985). This is normally done by finding the best fit between sap flux and environmental variables (Oren et al., 1998; Chuang et al., 2006). Here, the best fit between sap flux and VPD was achieved by shifting sap flux time series back by a half-hour. This short time-lag indicates little stem water storage which is in agreement with Phillips et al. (2003), who found water storage to be small in young ponderosa pine and to account only for 2–4% of daily water-use.

Canopy stomatal conductance (G_s) was calculated by a simplified form of the Penman–Monteith equation from T_{tree} following Monteith and Unsworth (2007):

$$G_s = \frac{K_G(T_a)T}{VPD} \quad (1)$$

where T is tree transpiration (g m^{-2}), VPD is vapor pressure deficit of the air (kPa), T_a is air temperature (°C) and K_G is the conductance coefficient (115.8 +0.4236T; kPa m^3 kg^{-1}), accounting for temperature effects on the psychometric constant, latent heat of vaporization, specific heat of air at constant pressure, and air density (Ewers and Oren, 2000). G_s values were converted from m^2 s^{-1} to mmol m^2 s^{-1} following Pearcy et al. (1989). This simplified form of the Penman–Monteith equation requires well-mixed conditions, when the boundary layer resistance is negligible and thus, VPD_a equals VPD_{leaf}. Indeed, given a daytime-average wind velocity of 3.1 ± 1.4 m s^{-1} and an average fascicle diameter of 1.6–2.1 mm, we estimated mean daytime leaf boundary layer conductance averaging 160 times G_s (Jones, 1992), indicating a high degree of canopy–atmosphere coupling. Moreover, for the same forest type, Irvine et al. (2002) found the degree of coupling was large during midday with the decoupling factor Ω averaging 0.05 (Jarvis and McNaughton, 1986). Therefore, we assumed it appropriate to use Eq. (1) for G_s estimates in this study. To keep relative errors of G_s < 10%, G_s was only calculated if VPD > 0.6 kPa (see Ewers and Oren, 2000).

To disentangle the effects of VPD and SWC on stomatal response of relatively isohydric ponderosa pine (Martinez-Vilalta et al., 2004), we determined stomatal sensitivities to VPD during the course of the summer dry season by fitting G_s to VPD under non-limiting light conditions (PAR ≥ 1200 μmol m^{-2} s^{-1}; Oren et al. (1999)):

$$G_s = b - a\ln(VPD) \quad (2)$$

where b is reference G_s at VPD = 1 kPa (G_{s-ref}) and a is the slope of the regression representing the sensitivity of G_s to VPD ($-dG_s/d\ln VPD$).

2.4.1. Photosynthesis

On the south-facing side of each tree, at about 1.8 m height, we choose two fascicles of current (2010 age-class) and previous year (2009 age-class) needles. We measured only south-facing sunlit needles as they exhibit similar conditions than the canopy and no differences in photosynthesis between north- and south-facing needles of *P. ponderosa* have been found (see Panek and Goldstein, 2001). Current-year needles were measured from 30 July onwards, when they were long enough to fit without damage inside the chamber. The same fascicles were measured throughout the experiment. Each measurement campaign lasted from 9:30 to 12:00 PST. Trees were measured in the same order, iterating between control and watered treatment. Photosynthesis (Pn_{leaf}), transpiration (T_{leaf}) and stomatal conductance (g_s) were measured at ambient CO_2 of 380 ppm under non-limiting light conditions (PAR = 1800 μmol m^{-2} s^{-1}: determined from light–response curves) with a Li-6400 equipped with a Li-6400-02B LED light source (Li-Cor, Lincoln, NB, USA). After clamping the needles in the chamber, we allowed the needles to acclimate and fluxes to stabilize for 2 min before measuring. Chamber temperature and relative humidity were set to mimic ambient conditions, resulting in an average relative humidity of 27.9 ± 4.2%, VPD_{leaf} of 2.8 ± 0.4 kPa and leaf temperature of 25.5 ± 1.7 °C.

Total leaf area was calculated by assuming each fascicle was a cylinder divided into n needles (Panek and Goldstein, 2001). We upscaled Pn_{leaf}, T_{leaf} and g_s rates (average of 2009 and 2010-age class needles; no significant differences between needle age-classes; *t*-test, $p = 0.68$) from m^2 leaf area to m^2 ground area by multiplying with overstory LAI (2× half-sided). LAI was estimated by optical techniques at the beginning and end of the summer season along two transects within the footprint area of the flux tower following methods in Law et al. (2001). We measured current-year needle elongation (on three fascicles at one branch per tree) with a caliper during each measurement campaign and visually determined needle loss from monthly tree photographs. Since we did not find a difference between treatments in current-year needle elongation (linear mixed effect models, treatment effect: $t = 0.72$, $p = 0.55$) we determined one site-specific LAI. In brief, LAI was interpolated for each measurement campaign from observations of current-year needle elongation and estimates of percentage needle loss of the three-year-old needles (2007-age-class) by assuming each needle-age class (i.e., 2007, 2008, 2009 and 2010) comprised 25% of the LAI at the end of the 2010 growing season.

2.4.2. Soil CO_2 efflux

Prior to manual and automated Rm and Rs_{tree} measurements, polyvinyl chloride (PVC) collars (manual: inside diameter of 10.1 cm, $n = 16$; automated: inside diameter of 20.3 cm, $n = 6$) were inserted 2 cm deep in all plots. For Rs_{tree} measurements the PVC collars were placed within 1 m south–west from the tree base, for Rm measurements the PVC collars were placed in the center of the plots in the open. Soil CO_2 efflux was measured at high temporal and spatial resolution as described in the following. Half-hourly measurements of Rs were made with an automated chamber system (Li-8100 with LI-8150 multiplexer and 8100-101 and 8100-104 chambers; Li-Cor, Lincoln, NB, USA) in three plots per treatment (Rs_{tree}: $n = 2$ and Rm: $n = 1$ per treatment). The length of one measurement period ranged between 60 and 90s (depending on efflux rates). Data coverage was about 70%, due to equipment and power failure, as well as omission of data that did not meet the quality criteria (coefficient of variation of flux computation < 2%). To cover the spatial variability of soil CO_2 efflux among plots and to estimate differences in Rs_{tree} and Rm, we measured soil CO_2 efflux with a closed manual chamber system (Li-6400; Li-Cor, Lincoln, NB, USA) at one location in each of the plots as follows. After placing the chamber on the PVC collar, [CO_2] was scrubbed to below ambient and then allowed to rise above ambient while soil CO_2 efflux was determined. Measurements were conducted bi-weekly between 14:00 and 16:00 PST. The CO_2 and H_2O zeros and spans of the Li-6400 and Li-8100 gas analyzers were calibrated before the beginning of the experiment, controlled monthly, and re-calibrated if the difference in zero gas was >2 ppm.

Power functions of Rs_{tree} and Rm (Knohl et al., 2008) showed that 9 of the 11 measurement campaigns were within 30% of the full population mean at the 95% confidence interval (CI), suggesting confidence in the precision of soil efflux estimates. For area scaling of Rs we first accounted for the area cover of trees vs. open area and weighted fluxes of Rs_{tree} and Rm accordingly. To up-scale automated Rs to the site-level, the regression between automated (campaign-days between 14:00 and 16:00) and manual Rs rates with a high precision (within 20% of the full population mean at the 95% CI) was used (see Fig. A.1; $y = 1.02x + 0.45$, $R^2 = 0.95$). Comparing site-level Rs to Reco (ecosystem respiration from night-time NEE) resulted in a ratio of 0.72 on average over the period studied (compare to 0.76 obtained by Law et al., 1999 in a forest close-by).

2.4.3. Gap-filling of EC and soil CO_2 efflux

Small data gaps (≤2 h) of continuous half-hourly flux measurements were substitute by linear interpolation, but only after estimation of model parameters for filling larger gaps. To fill larger data gaps (≥2 h) we proceeded as follows. First, Reco and Rs (Rs_{tree} and site-scaled automated measurements) were split in two SWC intervals (0–30 cm; threshold of 0.16 m^3 m^{-3}) and net ecosystem exchange (NEE) and evapotranspiration (ET) data were divided in monthly periods. Then, the data was filtered (4 × SD of 10-day intervals) to exclude extreme fluxes which are likely non-biological driven and therefore not accounted for in the models. Reco derived from night-time NEE estimates (PAR < 20 μmol m^{-2} s^{-1}) and Rs of each chamber was fitted to the following Lloyd–Taylor temperature response function in case SWC ≥ 0.16 $m^3 m^{-3}$:

$$\text{Reco, Rs} = R_{\text{ref}}\, e^{E_0((1/(T_{\text{ref}}-T_0))-(1/(T_m-T_0)))} \quad (3)$$

where R_{ref} is respiration under standard conditions (at T_{ref} = 10 °C), E_0 (K^{-1}) is the parameter for the activation energy, T_0 = −46.02 °C, as in the original Lloyd and Taylor model (Lloyd and Taylor, 1994) and T_m is the measured temperature (air or soil temperature, depending on best-model fit). For cases when SWC < 0.16 m^3 m^{-3} the Lloyd–Taylor model (Eq. (3)) was modified to account for the water limitation of respiration by substituting R_{ref} with

$$R_{\text{ref}} = (a\,\text{SWC} + b) \quad (4)$$

by assuming R_{ref} to be linearly dependent on SWC. Rs of the watered treatment was simply fitted to Eq. (3), as SWC was above 0.16 m^3 m^{-3} during most of the study.

Gross primary productivity (GPP) was estimated as

$$\text{GPP} = \text{NEE} - \text{Reco} \quad (5)$$

where NEE is daytime data only (PAR ≥ 20 μmol m^{-2} s^{-1}).

To fill day-time data gaps GPP was fit to a light–response model as in Falge et al. (2001) accounting for VPD limitations on photosynthesis (modified after Lasslop et al., 2010)

$$\text{GPP} = \frac{a\,\text{PAR}}{(1-(\text{PAR}/1800)) + ((a\,\text{PAR})/(A_{\max}\exp(-k\,\text{VPD}))} \quad (6)$$

where a is the ecosystem quantum yield (μmol CO_2 m^{-2} s^{-1}) and represents the initial slope of the light response curve, A_{max} is the maximum CO_2 uptake at light saturation (here at PAR = 1800 μmol m^{-2} s^{-1}), k is a dimensionless parameter for the sensitivity of GPP to changes in VPD. Because we found the parameter k was well constrained at low VPD, we did not include a VPD threshold as in Lasslop et al. (2010). To fill ET daytime data gaps,

we fitted a linear model of ET vs. potential evapotranspiration (see Thomas et al., 2009). Night-time ET data gaps were set to zero.

2.5. Statistics

To test overall differences in flux dynamics between treatments and to account for repeated measures in time, we used linear mixed effect models (lme) with treatment and time as fixed effects and plots as random effect, following Zuur et al. (2009). We also accounted for the autocorrelation structure at lag one for time series of continuous data. To test for differences in stomatal response to VPD between treatments, we assigned treatment and ln VPD as fixed effects and tree as random effects, allowing the intercept and the slope to vary between trees. We applied *t*-tests to test for differences in treatments at single measurement campaigns. For a better comparison of the variety of fluxes assessed, and to focus on flux dynamics in response to drought rather than on absolute numbers, we calculated fluxes relative to those of pre-drought conditions (20–24 June 2010) before initiation of the watering. Data processing and statistical analyses were performed using R 2.11.1 (R Development Core Team, 2010) with the nlme package for linear mixed effects models (Pinheiro et al., 2010).

3. Results

3.1. Effects of drought progression on CO_2 and H_2O fluxes

The spring of 2010 was exceptionally wet with 70.3 mm precipitation from May to mid June, exceeding the longterm average (1971–2000, PRISM Climate Group, Oregon State University) by about 50%, resulting in high SWC at the start of the dry season (Fig. 2b). Cold temperatures accompanied the spring rain, causing a late onset of bud break and needle elongation. Bud break occurred 18 June, almost 3 weeks later than the 4-year-average of 29 May at a nearby young pine site. After bud break and the end of the cold-wet weather period, ET and T_{tree} continued to increase, with the magnitude in T_{tree} tracking daily weather conditions (Fig. 2a and c). T_{tree} reached a maximum of 0.78 mm d^{-1} on 20 July and level off thereafter, then declining with SWC to below 50% at the end of August (Figs. 2b and c, and 3). GPP declined earlier than T_{tree} and ET in response to the drought. From mid July onwards, when SWC declined to 0.11 m^3 m^{-3} at 10 cm and 0.17 $m^3 m^{-3}$ at 30 cm depth, GPP remained below pre-drought conditions (Fig. 2b and d) while LAI continued to increase until mid August (data not shown). In fact, weekly GPP was strongly related to SWC (30 cm), decreasing by about 50% when SWC dropped from 0.22 to 0.11 m^3 m^{-3} (i.e., 88% and 19% REW; Fig. 3). This reduction in GPP was accompanied by an increase in the intrinsic water use efficiency (WUE_i = GPP/G_s; Fig. 3), nearly doubling between June and September (Table 1). The increase in WUE_i translates to a larger reduction in G_s than in GPP (Fig. 3). Consequently, resulting in a non-linear relationship of G_s with GPP (see also Fig. 6a). Although SWC was a strong driver of GPP and G_s, VPD exerted substantial control as seen in the tight coupling of half-hourly G_s with VPD (Fig. 4a). This VPD-induced response of G_s (and consequently control over GPP) was affected by soil water availability, as clearly seen by the decreasing sensitivity of G_s to VPD with drought progression (Fig. 4a).

Also soil surface CO_2 fluxes declined during the seasonal drought. Rs_{tree} (automated) generally followed patterns in T_{tree} dynamics, and both declined sharply when REW dropped below 40% (SWC of 0.14 m^3 m^{-3}; Figs. 2c and e, and 3). Interestingly, root-rhizosphere respiration ($Rr = Rs_{tree} - Rm$) was more sensitive to drought than microbial respiration in the control plots. While Rs_{tree} rates (both automated and manual) declined (Figs. 2e and 5a), Rm rates remained surprisingly constant (Fig. 5b), suggesting the

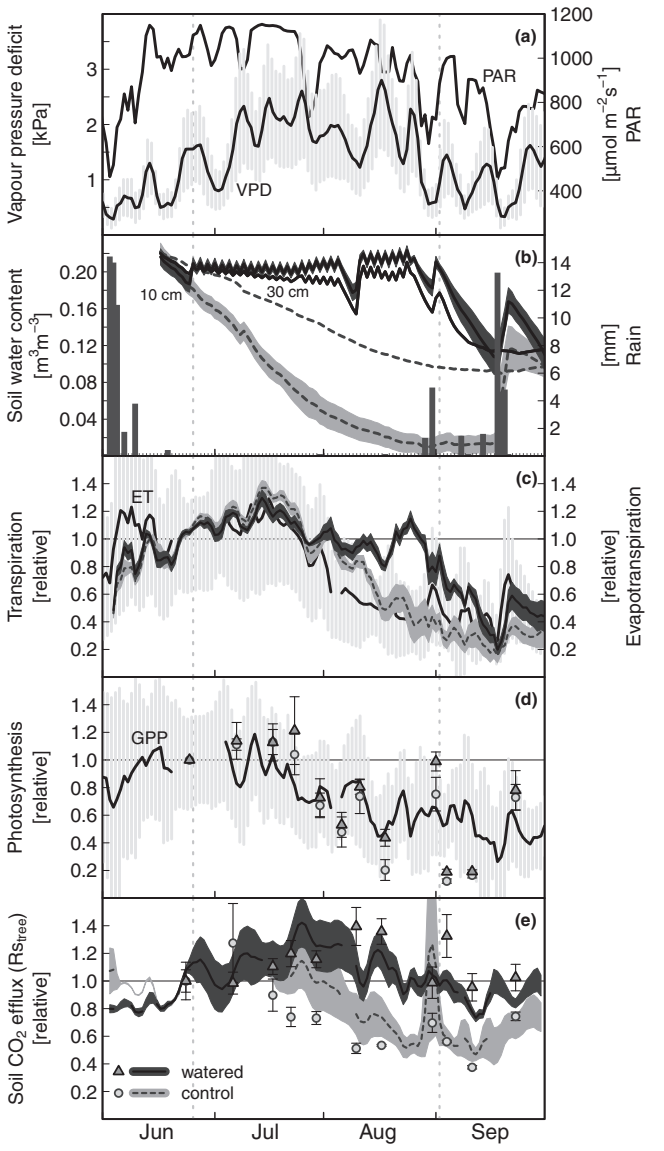

Fig. 2. Dynamics of atmospheric conditions and soil water content (SWC), as well as CO_2 and H_2O fluxes relative to pre-drought conditions during the summer 2010. (a) 3-day moving average of daytime vapor pressure deficit (VPD) and photosynthetic active radiation (PAR), (b) sum of daily precipitation and averaged daily SWC in 10 cm (n = 5) and 30 cm depth (n = 2) per treatment, (c) 3-day moving average of tree transpiration (T_{tree}) per treatment (n = 4) as well as evapotranspiration (ET), (d) 3-day moving average of gross primary production (GPP, dark gray line), as well as campaign-averages of net photosynthesis (Pn_{leaf}) per treatment (n = 5), and (e) averaged daily soil CO_2 efflux (Rs_{tree}) from automated (n = 2) and manual chambers (n = 5) for each treatment are shown. Longer data gaps (>1 d) are indicated by intermittent lines. Solid shaded areas and black error bars are ±1SE; gray vertical lines (VPD, ET, GPP) are ±1SD. The dashed vertical lines indicate the start (24 June) and end (31 August) of irrigation in the watered treatment.

reduction in Rs_{tree} was largely caused by highly water sensitive root-rhizosphere respiration ($Rr = Rs_{tree} - Rm$). Indeed, the contribution of Rr to Rs_{tree} declined with drought from 42% at the start of the dry season to 12% in August. (Fig. 5c and Table 1), and the reduction in Rr was linearly related to T_{tree} ($y = 2.52x - 0.33$; $R^2 = 0.58$, $p < 0.01$). In summary, this points towards a tight coupling of below- and aboveground tree dynamics in this semi-arid forest ecosystem.

3.2. Effects of watering on CO_2 and H_2O fluxes

Irrigation maintained SWC (0–30 cm) at about 0.20 m^3 m^{-3} (i.e., 70% REW) during July and August (see Table 1), so that SWC was 28%

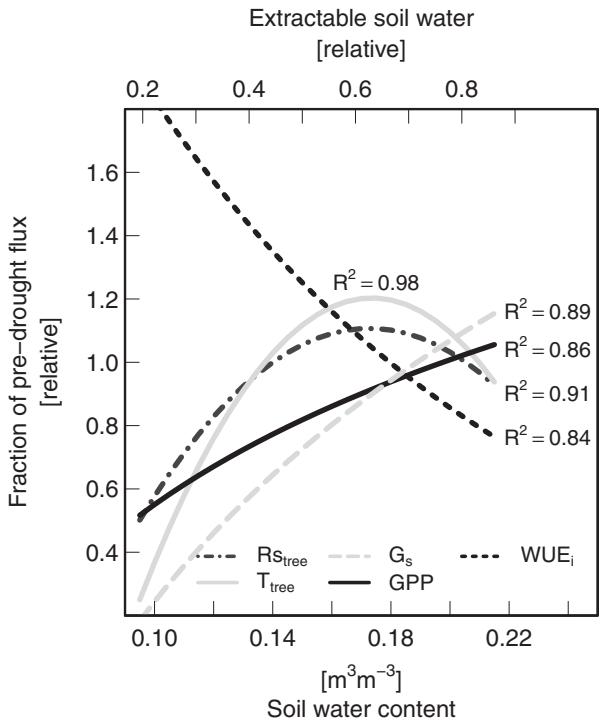

Fig. 3. Relationship of CO_2 and H_2O fluxes and intrinsic water-use efficiency (WUE_i) to SWC in 30 cm depth during summer drought. Fluxes and WUE_i are fractions relative to pre-drought conditions (20–24 June). Curves were fitted to 7-day (gap-filled) averages from mid June (after last major rain event, before onset of dry season) to mid September (before major rain event, partially recharging SWC), excluding days with rain and the following day. T_{tree}, GPP, G_s and WUE_i are day-time data only. The relationships with SWC were best explained by functions of different forms, GPP and G_s were expressed by a logarithmic function, WUE_i by an exponential function, T_{tree} and Rs_{tree} by a second-order polynomial function. See appendix (Fig. A.2) for data and regression models.

higher than the controls in July and 90% in August. Directly after irrigation (every other night to keep evaporative loss at a minimum) of 11 mm in June and July and 14.6 mm in August, SWC (0–30 cm) increased by about 0.015 $m^3\,m^{-3}$ and 0.025 $m^3\,m^{-3}$, respectively. This translates to about 4.5 and 7.5 mm of water remaining in the upper 30 cm of the soil, while about 6–7 mm should have infiltrated deeper in the soil, substantially re-wetting it to a depth of at least 60 cm. These pronounced changes in soil water content had albeit only a marginal effect on soil temperatures (measured at 10 cm depth) which were an average of 0.7 °C lower in the watered compared to the control treatment (Table 1).

Watering did not affect T_{tree} (Fig. 2c) and Pn_{leaf} (Fig. 2d) in July, when the difference in SWC (30 cm) between treatments was small (watered: 0.20 $m^3\,m^{-3}$, control: 0.17 $m^3\,m^{-3}$). As drought continued and REW in the watered compared to the control treatment more than doubled, Pn_{leaf} differed marginally between treatments at the end of August (17 August, control: 1.48 ± 0.50 μmol $CO_2\,m^{-2}\,s^{-1}$, watered: 3.49 ± 0.72 μmol $CO_2\,m^{-2}\,s^{-1}$, $t = 2.29$, $p = 0.055$; 31 August, control: 5.66 ± 0.85 μmol $CO_2\,m^{-2}\,s^{-1}$, watered: 7.73 ± 0.88 μmol $CO_2\,m^{-2}\,s^{-1}$, $t = 1.68$, $p = 0.131$). T_{leaf} and g_s followed similar dynamics, only slightly responding to increased water availability in August (data not shown).

The effect of watering on tree physiology became more clear when comparing T_{tree} rates (derived from sap flow measurements), which were significantly larger in the watered than the control trees during August and September (Table 2). Synchronously, G_s and G_{s-ref} differed between treatments (Fig. 4a and b, and Table 2). Moreover, watering not only maintained G_s and G_{s-ref}, but also the sensitivity of G_s to VPD (Fig. 4c and Table 2). This larger sensitivity of G_s to VPD ($-dG_s/d\ln$VPD) of watered compared to control trees caused differences in G_s between treatments to diminish at VPD > 3 kPa (Fig. 4a), thereby partly de-coupling G_s from soil water availability. This might explain the almost unchanged Pn_{leaf} rates in the watered compared to the control trees due to similar stomatal restrictions on assimilation caused by high VPD_{leaf} conditions (on average 2.8 ± 0.4 kPa) during leaf chamber measurements.

In contrast to the modest effect of watering on aboveground tree dynamics, soil CO_2 effluxes showed a much stronger, nearly instantaneous response to the irrigation (Fig. 5 and Table 3). The treatment effect increased from autotrophic to heterotrophic dominated respiration. Rm responded almost instantaneously to the watering, and compared to the control remained significantly higher during the entire treatment period (Fig. 5b; excluding 30 August, when the first summer rain along with colder temperatures affected soil CO_2 effluxes adversely). Rs_{tree} dynamics differed, initally responding only slightly to the watering, then increased to 54% higher than the control one month after the start of irrigation (Fig. 5a and Table 3). Rr was the least and last affected by the watering, and became significantly larger than the control only from mid August onwards (Fig. 5c and Table 3). This agrees well with the observed patterns in T_{tree} and G_s, indicating above- and belowground tree dynamics vary in-phase to changes in soil water availability.

3.3. Effects of soil water availability on the ecosystem C balance

To estimate the effects of soil water availability on the ecosystem C balance over the growing season (June–Sep 2010), we

Table 1
Monthly averages of daily weather conditions, amount of rain (control) and irrigation (watered), as well as relative soil water content (REW) and ecosystem fluxes for the control ('natural drought') and the watered treatment. Monthly means (of daily averages) ±1SD are given.

	June		July		August		September	
	Control	Watered	Control	Watered	Control	Watered	Control	Watered
VPD_{max} (kPa)	1.4 ±0.7		2.8 ±0.9		2.5 ±1.0		1.6 ±0.7	
Soil temperature (°C)	13.6 ±1.9	14.5 ±2.0	18.8 ±2.0	18.6 ±1.5	20.0 ±2.1	18.4 ±1.8	15.3 ±1.6	15.6 ±1.2
Rain/irrigation (mm)	46	41	0.1	169	6	227	25	0
REW (%)	80 ±4	81 ±4	60 ±0.09	75 ±2	30 ±7	71 ±9	19 ±1	36 ±10
T_{tree} (mm d^{-1})	0.48 ±0.12	0.61 ±0.15	0.62 ±0.10	0.73 ±0.07	0.35 ±0.10	0.58 ±0.08	0.19 ±0.05	0.30 ±0.11
G_s (mmol $m^{-2}\,s^{-1}$)	50.2 ±15.4	63.7 ±19.9	34.7 ±12.8	40.8 ±15.2	20.2 ±8.0	39.2 ±17.4	16.1 ±9.7	35.2 ±22.5
WUE_i (μmol $mmol^{-1}$)	172 ±45	–	210 ±54	–	269 ±91	–	296 ±132	–
GPP (g C $m^{-2}\,d^{-1}$)	4.5 ±0.7	–	4.3 ±0.8	–	2.8 ±0.7	–	1.9 ±0.7	–
GPP[a] (g C $m^{-2}\,d^{-1}$)	4.8 ±0.6	4.8 ±0.6	4.1 ±0.6	4.0 ±0.6	3.1 ±0.9	3.9 ±0.8	2.4 ±1	3.3 ±1.2
Rs (g C $m^{-2}\,d^{-1}$)	1.9 ±0.2	2.3 ±0.2	2.1 ±0.1	2.8 ±0.3	1.5 ±0.3	2.8 ±0.2	1.3 ±0.2	2.3 ±0.2
Rr/Rs_{tree}[b] (%)	42	40	40 ±14	26 ±4	12 ±8	28 ±12	13 ±6	32 ±4

[a] Modeled using the relationship of GPP and G_s given in Fig. 6.
[b] Fraction Rr/Rs_{tree} from campaign measurements (June, $n = 1$; July, $n = 4$; August, $n = 3$; September, $n = 3$.

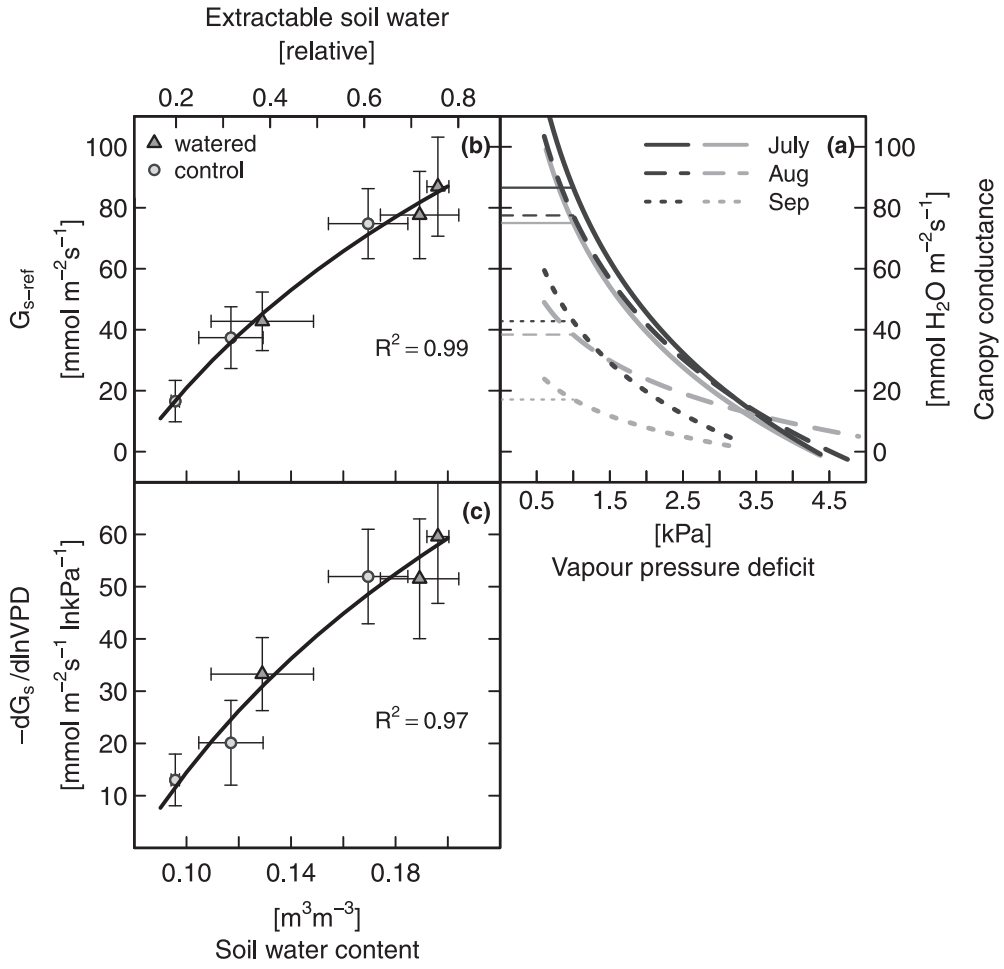

Fig. 4. Sensitivity of canopy conductance (G_s) to VPD for the control and the water treatment during the summer dry season (July–September). (a) Half-hourly G_s vs. VPD (VPD > 0.6 kPa and no rain) represented by curves of the best monthly model fit ($y = b - a \ln$ VPD; all curves are significant, see Table 2 for more details) with the horizontal lines indicating the intercept of the regressions (G_{s-ref}), (b) monthly G_{s-ref}, and (c) monthly $-dG_s/d \ln$ VPD (slope of the regression) vs. SWC (30 cm) are shown. The relationship of G_{s-ref} and $-dG_s/d \ln$ VPD with SWC are described by the following logarithmic functions: $G_{s-ref} = 240.6 + 95.4 \ln(SWC)$ and $-dG_s/d \ln VPD = 163.3 + 64.6 \ln(SWC)$.

estimated GPP for both treatments using the significant relationship of daily GPP with G_s in control trees (Fig. 6a). The derived seasonal C uptake (GPP_{Gs}) was 435 ± 39 g C m^{-2} for the control (compare to GPP of 413 g C m^{-2} derived from EC) and 487 ± 39 g C m^{-2} for the watered treatment. Watering therefore increased GPP_{Gs} by only 12% (Fig. 6b). This corresponds very well to the results from needle photosynthesis measurements which indicate a 14% increase averaged over the study period. Further the highly significant linear relationship between daytime ET and T_{tree} ($R^2 = 0.69$, $y = 3.4x + 0.86$) suggests that G_s rates derived from T_{tree} in a small number of trees should be relatively representative for the study area and thus can be used to upscale to the site-level. Comparing the increased C uptake of watered trees (+52 g C m^{-2}) with soil C loss derived from site-scaled soil CO_2 efflux measurements (+95 g C m^{-2}; watered: 311 ± 47 g C m^{-2} vs. control: 216 ± 32 g C m^{-2}) indicates that increased water availability affected belowground fluxes more strongly than photosynthesis. This larger effect of watering on site-scaled automated Rs is also in agreement with campaign measurements that indicate an overall treatment effect of 48%. In summary, increased soil water availability during otherwise hot dry summers potentially negatively affects the short-term seasonal NEE due to a larger response of soil CO_2 efflux than photosynthesis (assuming a positive or no response of aboveground respiration on the watering).

4. Discussion

We observed a tight coupling of carbon and water dynamics in a young ponderosa pine stand during the summer dry season. The magnitude of component ecosystem CO_2 and H_2O fluxes was closely linked to soil water availability (Fig. 3) and atmospheric water deficit (Fig. 4). Nevertheless, component fluxes differed in their sensitivity to the summer drought and were affected differently by artificially increased water availability (e.g., Fig. 5). In the following, we will discuss the progression of drought and effects of watering in the context of (1) carbon and water coupling, (2) belowground vs. aboveground flux dynamics and (3) water availability and C balance.

4.1. Coupling of carbon and water dynamics

Water and carbon fluxes were as hypothesized tightly coupled, nevertheless they differed in their drought sensitivity. After onset of the dry season flux dynamics markedly differed with a decline in G_s and GPP, while T_{tree} and Rs_{tree} continued to increase. The observed initial increase in T_{tree} was mainly caused by higher evaporative demand of the atmosphere and to some extend by an increase in leaf area. Transpiration rates in young *P. ponderosa* are found to be generally high when not limited by soil water availability (Irvine et al., 2002, 2004). Nevertheless, isohydric tree species, such

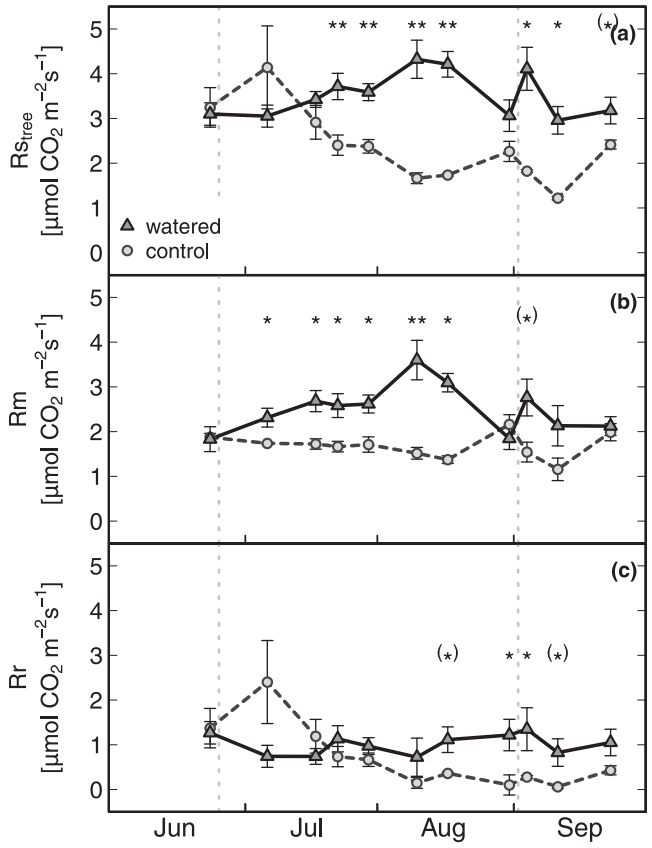

Fig. 5. Dynamics of soil CO_2 efflux, (a) in close proximity to the trees (Rs_{tree}; <1 m), (b) in the open (Rm; >5 m away from trees) and (c) root-rhizosphere respiration (Rr) estimated as difference between Rs_{tree} and Rm. The significance levels of the *t*-tests between treatments at each time point are given ((∗) $0.1 \geq p > 0.05$; ∗ $0.05 \geq p > 0.01$; ∗∗ $0.01 \geq p > 0.001$). The dashed vertical lines indicate the start and end of irrigation in the watered treatment.

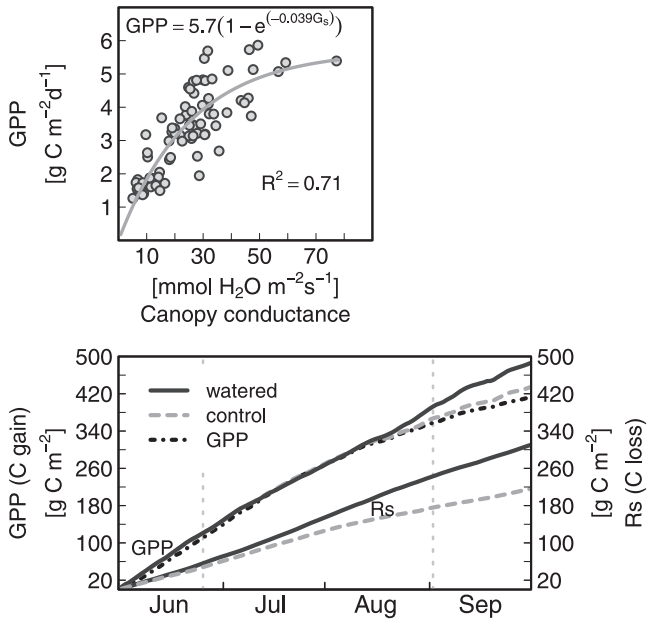

Fig. 6. Ecosystem net photosynthesis (GPP) in relation to canopy conductance and cumulative C gain and loss for both treatments. (a) GPP (only if non-gapfilled GPP $n > 12\,d^{-1}$) vs. mean G_s (VPD > 0.6 kPa and excluding rain events) of control trees fitted with an exponential saturation model, and (b) cumulative soil C loss (Rs, $n = 3$ per treatment, upscaled to site-level) as well as ecosystem C gain for both treatments estimated from the relation of average G_s with daily sums of GPP (see panel a), and 'normal' cumulative GPP (dashed black line) are shown. Please note, we accounted for slightly higher G_s of watered trees prior irrigation and multiplied G_s by 0.80 before deriving estimates of GPP for the watered treatment. The dashed vertical lines indicate the start and end of irrigation in the watered treatment.

as ponderosa pine, tightly regulate stomatal conductance to limit excessive water loss and maintain relatively high leaf water potentials to protect the xylem from cavitation (Martinez-Vilalta et al., 2004). This tight regulation of stomatal conductance may explain the decline of weekly-averaged G_s early in the season while no reduction in G_{s-ref} and $-dG_s/d\ln VPD$ occurred (between June and July, Table 2). The lack of a treatment effect in response to the irrigation in T_{tree} and G_s at this early stage of the drought (difference in SWC was $0.03\,m^3\,m^{-3}$ between treatments) indicates that soil water was not the limiting factor. Thus, the slight decline of GPP at this initial phase of the dry season should be largely due to VPD induced stomatal restrictions on C uptake. However, we can not totally exclude effects on GPP by early soil water limitation in shallow rooting herbs and grasses (i.e., REW in 10 cm depth dropped from 55% to 25% between 1 and 15 July), which had senesced by the end of July. Because grasses were sparse and generally low in productivity (approx. $16\,g\,C\,m^{-2}\,y^{-1}$, measured at young pine site close-by) there was likely no noticeable effect of grass senescence on ecosystem C uptake, contrary to findings commonly reported in other Mediterranean forest ecosystems with dense grass coverage (e.g., Unger et al., 2009).

Due to the relatively late start of the dry season, pronounced drought effects on ecosystem fluxes occurred only at the beginning of August and were likely driven by a continuous decline in soil water availability. In contrast, Goldstein et al. (2000) suggested for a young ponderosa pine plantation that extreme hot days may have led to cavitation, causing a reduction in ET and GPP that was

Table 2
Results of the linear mixed effects models to test for treatment differences in daily T_{tree} ($mm\,d^{-1}$) and in the sensitivity of half-hourly G_s to ln VPD. Means, 95% confidence intervals (CI_{95}, 1.96 times SE) and *t*-values of fixed effects for separate monthly models are shown. The treatment term represents the difference of the intercept and the interaction term represents the difference in the slope of the regressions. In case of T_{tree} the slope represents the time course. In case of G_s the intercept represents G_{s-ref}, (G_s at VPD = 1 kPa) and the slope the sensitivity of G_s to lnVPD ($-dG_s/d\ln VPD$). Significant *t*-values are in bold. Time is in days.

	June			July			August			September		
	Mean	±CI_{95}	*t*	Mean	±CI_{95}	*t*	Mean	±CI_{95}	*t*	Mean	±CI_{95}	*t*
Transpiration (T_{tree})												
Intercept	0.56	±0.14	**8.01**	0.70	±0.20	**7.33**	0.88	±0.22	**8.15**	0.10	±0.29	0.65
Treatment	0.14	±0.20	1.40	0.09	±0.25	0.66	−0.12	±0.29	−0.81	0.62	±0.41	**2.99**
Time	0.01	±0.00	**6.73**	0.00	±0.00	**−2.45**	−0.01	±0.00	**−6.58**	0.00	±0.00	0.66
Treatment × time	0.00	±0.00	0.29	0.00	±0.00	0.54	0.01	±0.00	**3.14**	−0.01	±0.00	**−2.57**
Stomatal conductance (G_s)												
Intercept	65.01	±16.76	**7.60**	74.79	±22.52	**6.51**	39.33	±19.50	**3.95**	16.58	±13.31	**2.44**
Treatment	16.06	±23.70	1.33	12.14	±31.83	0.75	38.29	±27.58	**2.72**	26.18	±18.82	**2.73**
VPD	−53.41	±17.19	**−6.09**	−51.94	±17.72	**−5.74**	−22.18	±15.70	**−2.77**	−13.02	±9.70	**−2.63**
Treatment × VPD	−14.24	±24.30	−1.15	−7.64	±25.07	−0.60	−29.32	±22.17	**−2.59**	−20.25	±13.70	**−2.90**

Table 3
Results of the linear mixed effects models to test for treatment differences in soil CO_2 effluxes and Pn_{leaf} over the time course of the experiment. Means, 95% confidence intervals (CI_{95}, 1.96 times SE) and *t*-values of fixed effects are given. The treatment term represents the difference of the intercept and the interaction term represents the difference in the slope (different variation with time) of the regressions. Significant *t*-values are in bold. Time is in days.

	Rs			Rm			Rr			Pn_{leaf}		
	Mean	$\pm CI_{95}$	*t*	Mean	$\pm CI_{95}$	*t*	Mean	$\pm CI_{95}$	*t*	Mean	$\pm CI_{95}$	*t*
Intercept	3.28	±0.58	**11.08**	1.66	±0.53	**6.18**	1.08	±0.46	**4.64**	8.77	±1.71	**10.06**
Treatment	0.38	±0.81	0.91	1.20	±0.75	**3.13**	−0.30	±0.63	−0.94	0.46	±2.41	0.37
Time	−0.02	±0.01	**−4.31**	0.00	±0.01	−0.03	−0.01	±0.01	**−3.80**	−0.08	±0.03	**−5.54**
Treatment × time	0.02	±0.01	**2.80**	−0.01	±0.01	−1.09	0.02	±0.01	**3.77**	0.01	±0.03	0.31

sustained over the summer season. Here, we clearly found tree C uptake to be limited by water availability, as can be seen by the decline of G_{s-ref} and $-dG_s/d\ln VPD$ with soil water content. Interestingly, the relationship of G_{s-ref} and $-dG_s/d\ln VPD$ with SWC appears to be identical in both treatments (i.e., shown by the single-response lines; Fig. 4b and c), with a strong decline at REW <50%, confirming a pivotal role of water availability on stomatal control. Moreover, the observed threshold for water-limitation at about 40–50% REW seems consistent for a wide range of forest ecosystems (Breda et al., 2006; Granier et al., 2007; Domec et al., 2009), and may emerge as a general rule of thumb to identify forests under drought stress.

Simultaneously with soil water-stress, we found the ecosystem's water loss to be restricted more than C uptake and release, causing the WUE_i to increase (Fig. 3). Similar patterns have been observed in a young ponderosa pine plantation close-by where the inherent WUE (calculated as GEP times VPD divided by ET) was found to more than double during the seasonal summer drought over the 5 years measured (Vickers et al., 2012). The non-linear relationship between assimilation and conductance has often been observed to increase WUE, since water loss is being restricted more than the inhibition of photosynthesis (Chaves et al., 2003). Thus, changes in G_s under water-limiting conditions (G_s < 25 mmol m^{-2} s^{-1}) should affect GPP relatively more than at unstressed conditions and large G_s. Hence, slight weather changes that dampen drought severity (i.e., small rain events, increased cloudiness) may increase stomatal conductance and largely affect C uptake, e.g., as seen at the end of August, when two hot-dry days (VPD of 2.7 kPa) were followed by two cooler days (VPD of 1.1 kPa: PAR > 900 μmol m^{-2} s^{-1}) and GPP more than doubled (from 2.5 to 6.6 μmol CO_2 m^{-2} s^{-1}). In addition, small rain events (1 and 5 mm on 29 and 31 August) affected CO_2 fluxes, causing a pulse of CO_2 from the soils and a stimulation of photosynthesis (see Fig. 2). While soil microbes were affected directly by the increase in soil water (see Jarvis et al., 2007), the response of photosynthesis was very likely caused by positive effects of low VPD on G_s rather than increased soil water availability, as only the very shallow soil layers were re-wetted during the rain event. VPD effects occurring along with rain events, especially in isohydric species, should be considered when interpreting responses of semi-arid ecosystems to rain pulse events.

4.2. Above- and belowground coupling

Often, during drought, assimilation rates are found to decrease more strongly than respiration, so that ecosystems can become a CO_2 source to the atmosphere (Schwalm et al., 2009). Here, we found Rs_{tree} to be less affected than GPP early in the summer dry season, and Rs_{tree} continued to increase while GPP began declining. However, later in the season with increasing drought severity the picture changed and relative fluxes of Rs_{tree} and GPP were reduced to a similar extend.

Root-rhizosphere respiration seemed to be the main determinant for the strong decline in soil CO_2 efflux during drought, while microbial respiration only slightly decreased (Fig. 5b and c). The apparently drought-insensitivity of Rm is also reported elsewhere (Lavigne et al., 2004; Irvine et al., 2008), but is in contrast to other studies (e.g., Borken et al., 2006), and contradicts the strong response of Rm to the watering in our study. In a mature ponderosa pine forest close-by, Irvine et al. (2008) concluded that soil water constraints on decomposition might be compensated by a simultaneously strong increase in temperature. In the relatively open forest we studied, shallow soil temperatures increased during summer and reached as much as 45 °C. Also high solar irradiance, facilitating decomposition by breaking down larger organic compounds to smaller molecules (e.g., Gallo et al., 2006) may be another explanatory factor largely masking water constrains on decomposition. The degree of water-limitation on decomposition becomes clearer, considering the response of Rm under well-watered conditions. Just shortly after the start of the watering, when shallow SWC (10 cm depth) differed by only 0.06 m^3 m^{-3} between treatments (control: 0.14 m^3 m^{-3} vs. watered: 0.20 m^3 m^{-3}), Rm rates in the watered treatment were already significantly increased, translating to a RWC threshold of Rm at about 50% for the upper 10 cm of soil. With further drying of the soil (control: 0.03 m^3 m^{-3} vs. watered: 0.20 m^3 m^{-3}), Rm rates in the watered compared to the control treatment more than doubled. Constantly higher Rm rates under watering point towards sufficient amounts of labile soil C to be available, largely preserved from decomposition under "normal" water-limiting summer conditions (Kelliher et al., 2004). This is confirmed by Noormets et al. (2010) who found years with wetter climate to have higher Rm rates and soil C loss compared to drought years in a loblolly pine plantation. Longer-term studies over multiple years of water manipulations indicate a continuing effect on soil C dynamics. In the fifth year of summer irrigation, Rs was increased by 58% in the wet compared to the control treatment in a Mediterranean woodland (Cotrufo et al., 2011), and after 13-years of precipitation manipulations soil C stocks in the O horizon were lower under wet vs. control and dry conditions (Froberg et al., 2008). In summary, this clearly demonstrates soil CO_2 loss to be restricted by low soil moisture, and highlights a possible risk of reducing soil C stocks due to larger decomposition under moist and warm conditions, if not compensated by increased plant C inputs.

Confirming our second hypothesis, the trend in root-rhizosphere respiration followed largely aboveground tree dynamics. Rr rates remained relatively stable in the watered treatment but decreased in the control along with progressing drought (Fig. 5c). Root-rhizosphere respiration in young ponderosa pine should be largest under favorable growing conditions when carbohydrate supply is high (C source) and the C demand of roots is large (C sink). In fact, fine root growth in young ponderosa pine is largest in early summer with a peak in fine root biomass between late July and beginning of August (Andersen et al., 2008). Hence, when the C sink strength is reduced along with a reduction in C supply, this may lead to a larger reduction in Rr later in the growing season. Less available C from photosynthesis, as seen by the concurrent drop in GPP, together with a longer retention time of

carbohydrates in leaves, reduces belowground C allocation and exudation under drought conditions (Ruehr et al., 2009), which should indeed cause root and microbial-rhizosphere respiration to be decreasing. The significantly higher Rr rates in the watered treatment in late summer, which occurred simultaneously with increased T_{tree} and G_s in the watered trees, point towards sufficient amounts of carbohydrates being available and allocated to the root system for maintenance and root growth. This result is in agreement with findings of Irvine et al. (2005) made on young pines that were watered on one side compared to control trees during summer drought. They concluded that changes in assimilation rates between treatments were mainly responsible for the observed differences in Rr rates. In fact, the significant linear relationship of Rr with daily T_{tree} as observed in our study and reported from a mature ponderosa pine forest (Irvine et al., 2008), adds evidence for a tight control of aboveground tree dynamics on belowground processes in these semi-arid pine systems.

One might speculate that lower soil water availability (i.e., less winter/spring precipitation) at the onset of the seasonal drought reduces the length of favorable growing conditions, inhibits root growth earlier in the season which further amplifies tree water-stress, and may ultimately carry over into the following year. Carry-over effects, following severe or multi-year drought have been observed to impact the carbon and water cycle in ponderosa pine forests (Thomas et al., 2009), however, an in-depth understanding of the role of belowground processes has yet to emerge.

4.3. Effects of water availability on C balance

The significant relationship of GPP with G_s during natural summer drought gave us the opportunity to estimate ecosystem C uptake under well-watered conditions. We assumed the same G_s vs. GPP relationship applies to watered trees, hence presumed no changes in photosynthetic capacity. In a study on young ponderosa pine trees during mild summer drought, irrigated trees were found to have a slightly higher photosynthetic capacity than control trees, likely caused by increased nitrogen uptake of watered trees (Panek and Goldstein, 2001). Leaf nitrogen concentrations (measured on current year and last year needles at the end of the experiment), however, did not differ between treatments in our study ($p = 0.30$; control: $1.24\% \pm 0.04$; $1.30\% \pm 0.03$). Moreover, consensus has emerged that the limitation of CO_2 diffusion due to stomatal closure and reduced mesophyll conductance is the main cause of decreased photosynthesis under water stress conditions (Flexas et al., 2004). This seems to confirm our approach of deriving estimates on C uptake from stomatal conductance. Although derived GPP_{Gs} of the watered treatment was 12% larger than under control conditions during the study period (June–September), this was largely offset by the strong increase of Rm in response to the irrigation as discussed above. However, longer-term effects are less clear. Modeling exercises find that productivity generally increases along with more precipitation and higher temperatures, as net primary production is stimulated more than decomposition (Luo et al., 2008). Indeed, multiyear water manipulation experiments indicate plant productivity increases with water availability (Cotrufo et al., 2011; Metcalfe et al., 2010). In contrast, the net effect on soil C is less distinct. Some studies find the net effect on soil C to be zero (the effect on soil input and output balance each other; Cotrufo et al., 2011) while others find it to be negative (higher soil C content under drought compared to control/wet conditions; Sardans et al., 2008; Froberg et al., 2008). To allow predictions of net effects on the C balance under future conditions, a more thorough understanding of the contrasting responses of tree and soil C dynamics to water availability is clearly needed.

5. Conclusions

We studied the coupling of component ecosystem CO_2 and H_2O fluxes in relation to soil water content (SWC) and atmospheric water deficit (VPD) under natural summer drought and irrigation in a post-fire regenerating young ponderosa pine stand. Carbon and water fluxes were tightly coupled and strongly decreased as drought progressed. As hypothesized, above- and belowground tree fluxes were in-phase as seen by the concurrent decline in root-rhizosphere respiration along with GPP and T_{tree} as drought progressed, while watering largely maintained Rr along with T_{tree} and G_s. In contrast to our hypothesize, net carbon uptake appears to be higher under natural summer drought than under well-watered conditions, because microbial respiration increased more than photosynthesis with water additions. This clearly highlights the importance of understanding the dissimilar response of tree and soil dynamics when estimating C sequestration potential in water-limited forest ecosystems. Further, while soil water availability was the major driver of seasonal trends in flux dynamics, VPD induced daily changes in G_s that affected T_{tree} and photosynthesis, with the sensitivity of G_s to VPD being in turn controlled by soil water availability. These short- and long-term dynamics should be considered in future water manipulation studies and accounted for interactively in ecosystem process models when predicting impacts on ecosystems to future climate conditions.

Acknowledgments

This research was supported by the Office of Science (BER), US Department of Energy (Award DE SC0005322), and a Leopoldina Research Fellowship to NKR (LPDS 2009-37). We like to thank the Oregon Department of Forestry in Sisters, OR for their outstanding support, K. Davis and M. Trappe for maintaining the flux tower, C. Pettijohn for installing sap flux sensors, as well as C. Thomas and D. Vickers for flux tower data processing.

Appendix A.

See Appendix Figs. A.1 and A.2.

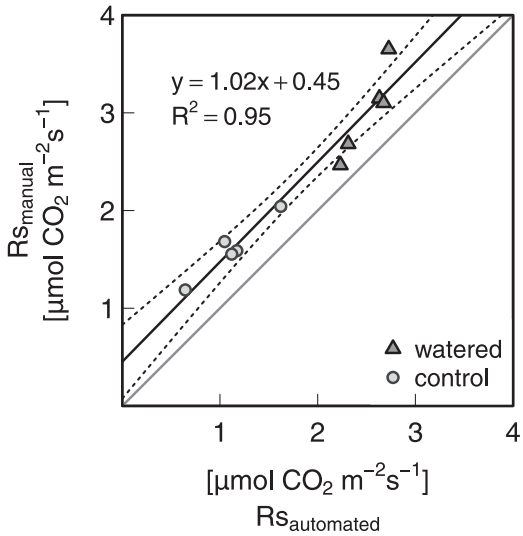

Fig. A.1. Relationship of Rs from manual and automated measurements. The Rs average is calculated from weighted Rs_{tree} and Rm measurements accordingly to spatial cover of trees vs. open area. Campaign-averages of manual Rs are within 20% precision at the 95% confidence interval. The thin gray line is the one-to-one line. The dashed lines represent the 95% confidence interval of the regression. The offset from the one-to-one line suggest that the automated chambers do not directly provide an estimate of site Rs.

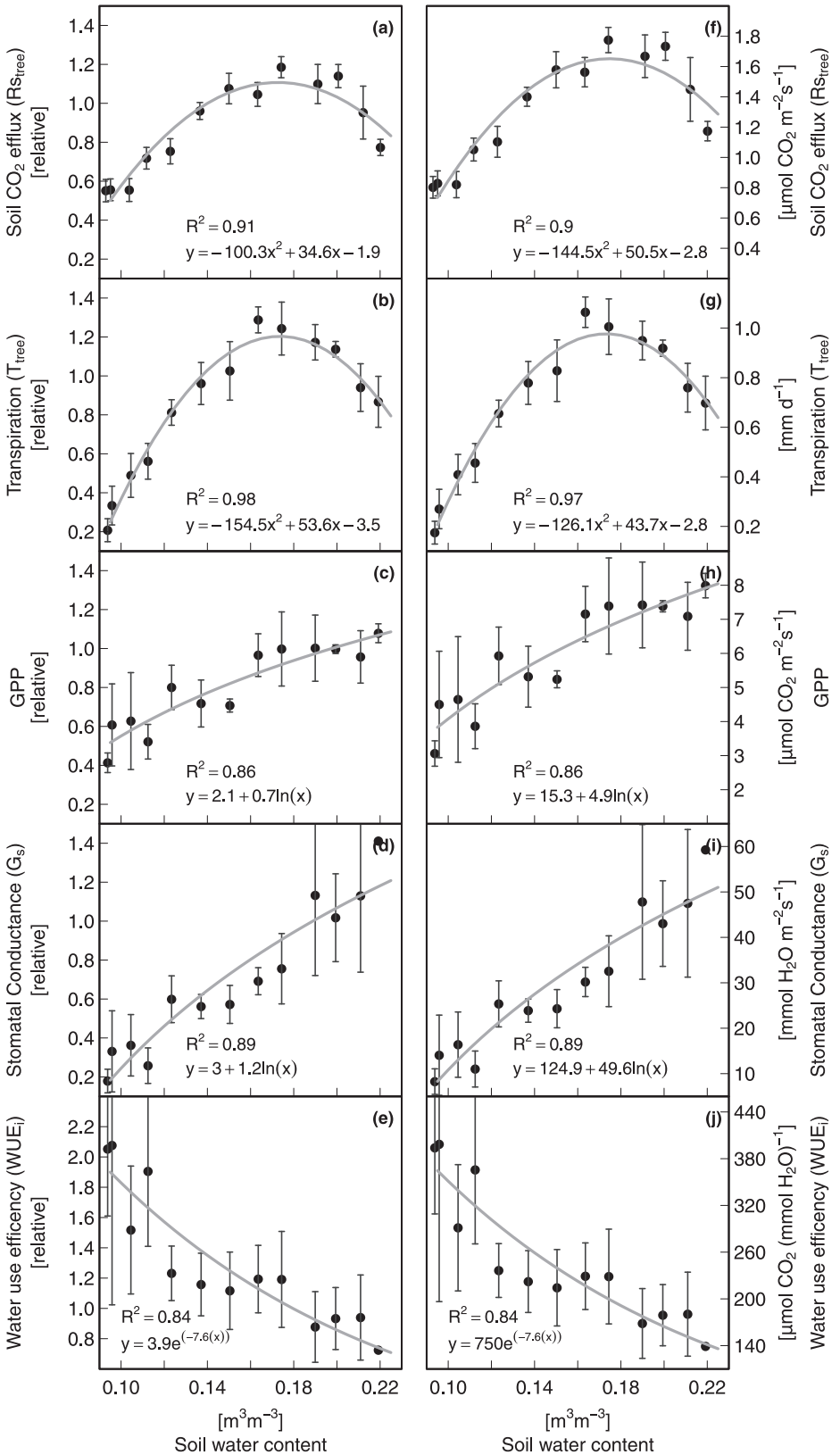

Fig. A.2. CO_2 fluxes, transpiration, stomatal conductance G_s and intrinsic water-use efficiency (WUE_i) in relation to SWC in 30 cm depth. Data points are 7-day gap-filled averages from mid June (after last major rain event, before onset of dry season) to mid September (before major rain event partly recharging SWC), excluding rainy days plus the following day. (a–e) Rs, T_{tree}, GPP and G_s relative to pre-drought conditions (20—24 June), and (f–j) rates of Rs, T_{tree}, GPP, G_s and WUE_i in relation to SWC are given. T_{tree}, GPP, G_s and WUE_i are day-time only.

References

Andersen, C.P., Phillips, D.L., Rygiewicz, P.T., Storm, M.J., 2008. Fine root growth and mortality in different-aged ponderosa pine stands. Can. J. Forest Res. 38 (7), 1797–1806.

Atkin, O.K., Macherel, D., 2009. The crucial role of plant mitochondria in orchestrating drought tolerance. Ann. Bot. 103 (4), 581–597.

Borken, W., Savage, K., Davidson, E.A., Trumbore, S.E., 2006. Effects of experimental drought on soil respiration and radiocarbon efflux from a temperate forest soil. Glob. Change Biol. 12 (2), 177–193.

Breda, N., Huc, R., Granier, A., Dreyer, E., 2006. Temperate forest trees and stands under severe drought: a review of ecophysiological responses, adaptation processes and long-term consequences. Ann. Forest Sci. 63 (September (6)), 625–644.

Brooks, J., Meinzer, F., Coulombe, R., Gregg, J., 2002. Hydraulic redistribution of soil water during summer drought in two contrasting pacific northwest coniferous forests. Tree Physiol. 22 (15–16), 1107–1117.

Brumme, R., 1995. Mechanisms of carbon and nutrient release and retention in beech forest gaps III. Environmental-regulation of soil respiration and nitrous-oxide emissions along a microclimatic gradient. Plant Soil 169, 593–600.

Chaves, M., Maroco, J., Pereira, J., 2003. Understanding plant responses to drought – from genes to the whole plant. Funct. Plant Biol. 30 (3), 239–264.

Chuang, Y., Oren, R., Bertozzi, A., Phillips, N., Katul, G., 2006. The porous media model for the hydraulic system of a conifer tree: linking sap flux data to transpiration rate. Ecol. Model. 191 (3–4), 447–468.

Cotrufo, M.F., Alberti, G., Inglima, I., Marjanovic, H., LeCain, D., Zaldei, A., Peressotti, A., Miglietta, F., 2011. Decreased summer drought affects plant productivity and soil carbon dynamics in a mediterranean woodland. Biogeosciences 8 (9), 2729–2739.

Domec, J., Warren, J., Meinzer, F., Brooks, J., Coulombe, R., 2004. Native root xylem embolism and stomatal closure in stands of douglas-fir and ponderosa pine: mitigation by hydraulic redistribution. Oecologia 141 (1), 7–16.

Domec, J.-C., Noormets, A., King, J.S., Sun, G., McNulty, S.G., Gavazzi, M.J., Boggs, J.L., Treasure, E.A., 2009. Decoupling the influence of leaf and root hydraulic conductances on stomatal conductance and its sensitivity to vapour pressure deficit as soil dries in a drained loblolly pine plantation. Plant Cell Environ. 32 (8), 980–991.

Ewers, B., Oren, R., 2000. Analyses of assumptions and errors in the calculation of stomatal conductance from sap flux measurements. Tree Physiol. 20 (9), 579–589.

Falge, E., Baldocchi, D., Olson, R., Anthoni, P., Aubinet, M., Bernhofer, C., Burba, G., Ceulemans, R., Clement, R., Dolman, H., Granier, A., Gross, P., Grunwald, T., Hollinger, D., Jensen, N., Katul, G., Keronen, P., Kowalski, A., Lai, C., Law, B., Meyers, T., Moncrieff, H., Moors, E., Munger, J., Pilegaard, K., Rannik, U., Rebmann, C., Suyker, A., Tenhunen, J., Tu, K., Verma, S., Vesala, T., Wilson, K., Wofsy, S., 2001. Gap filling strategies for defensible annual sums of net ecosystem exchange. Agric. Forest Meteorol. 107 (1), 43–69.

Flexas, J., Bota, J., Loreto, F., Cornic, G., Sharkey, T., 2004. Diffusive and metabolic limitations to photosynthesis under drought and salinity in C-3 plants. Plant Biol. 6 (May (3)), 269–279.

Froberg, M., Hanson, P.J., Todd, D.E., Johnson, D.W., 2008. Evaluation of effects of sustained decadal precipitation manipulations on soil carbon stocks. Biogeochemistry 89 (2), 151–161.

Gallo, M.E., Sinsabaugh, R.L., Cabaniss, S.E., 2006. The role of ultraviolet radiation in litter decomposition in arid ecosystems. Appl. Soil Ecol. 34 (1), 82–91.

Gerten, D., Luo, Y., Le Maire, G., Parton, W.J., Keough, C., Weng, E., Beier, C., Ciais, P., Cramer, W., Dukes, J.S., Hanson, P.J., Knapp, A.A.K., Linder, S., Nepstad, D., Rustad, L., Sowerby, A., 2008. Modelled effects of precipitation on ecosystem carbon and water dynamics in different climatic zones. Glob. Change Biol. 14 (10), 2365–2379.

Goldstein, A., Hultman, N., Fracheboud, J., Bauer, M., Panek, J., Xu, M., Qi, Y., Guenther, A., Baugh, W., 2000. Effects of climate variability on the carbon dioxide, water, and sensible heat fluxes above a ponderosa pine plantation in the sierra nevada (ca). Agric. Forest Meteorol. 101 (March (2–3)), 113–129.

Granier, A., 1987. Sap flow measurements in douglas-fir tree trunks by means of a new thermal method. Ann. Sci. Forest. 44 (1), 1–14.

Granier, A., Biron, P., Lemoine, D., 2000. Water balance, transpiration and canopy conductance in two beech stands. Agric. Forest Meteorol. 100 (4), 291–308.

Granier, A., Reichstein, M., Breda, N., Janssens, I.A., Falge, E., Ciais, P., Gruenwald, T., Aubinet, M., Berbigier, P., Bernhofer, C., Buchmann, N., Facini, O., Grassi, G., Heinesch, B., Ilvesniemi, H., Keronen, P., Knohl, A., Koestner, B., Lagergren, F., Lindroth, A., Longdoz, B., Loustau, D., Mateus, J., Montagnani, L., Nys, C., Moors, E., Papale, D., Peiffer, M., Pilegaard, K., Pita, G., Pumpanen, J., Rambal, S., Rebmann, C., Rodrigues, A., Seufert, G., Tenhunen, J., Vesala, I., Wang, Q., 2007. Evidence for soil water control on carbon and water dynamics in European forests during the extremely dry year: 2003. Agric. Forest Meteorol. 143 (1–2), 123–145.

Hanson, P., Weltzin, J., 2000. Drought disturbance from climate change: response of United States forests. Sci. Total Environ. 262 (3), 205–220.

Irvine, J., Law, B., Anthoni, P., Meinzer, F., 2002. Water limitations to carbon exchange in old-growth and young ponderosa pine stands. Tree Physiol. 22 (2–3), 189–196.

Irvine, J., Law, B., Kurpius, M., Anthoni, P., Moore, D., Schwarz, P., 2004. Age-related changes in ecosystem structure and function and effects on water and carbon exchange in ponderosa pine. Tree Physiol. 24 (7), 753–763.

Irvine, J., Law, B.E., Kurpius, M.R., 2005. Coupling of canopy gas exchange with root and rhizosphere respiration in a semi-arid forest. Biogeochemistry 73 (1), 271–282.

Irvine, J., Law, B.E., Martin, J.G., Vickers, D., 2008. Interannual variation in soil CO_2 efflux and the response of root respiration to climate and canopy gas exchange in mature ponderosa pine. Glob. Change Biol. 14 (12), 2848–2859.

Jarvis, P., McNaughton, K., 1986. Stomatal control of transpiration – scaling up from leaf to region. Adv. Ecol. Res. 15, 1–49.

Jarvis, P., Rey, A., Petsikos, C., Wingate, L., Rayment, M., Pereira, J., Banza, J., David, J., Miglietta, F., Borghetti, M., Manca, G., Valentini, R., 2007. Drying and wetting of Mediterranean soils stimulates decomposition and carbon dioxide emission: the "Birch effect". Tree Physiol. 27, 929–940.

Jentsch, A., Beierkuhnlein, C., 2008. Research frontiers in climate change: effects of extreme meteorological events on ecosystems. C. R. Geosci. 340 (9–10), 621–628.

Jones, H.G., 1992. Plants and Microclimate: A Quantitative Approach to Environmental Plant Physiology. Cambridge University Press, Cambridge, UK.

Kelliher, F., Ross, D., Law, B., Baldocchi, D., Rodda, N., 2004. Limitations to carbon mineralization in litter and mineral soil of young and old ponderosa pine forests. Forest Ecol. Manage. 191 (1–3), 201–213.

Knohl, A., Soe, A.R.B., Kutsch, W.L., Goeckede, M., Buchmann, N., 2008. Representative estimates of soil and ecosystem respiration in an old beech forest. Plant Soil 302, 189–202.

Lasslop, G., Reichstein, M., Papale, D., Richardson, A.D., Arneth, A., Barr, A., Stoy, P., Wohlfahrt, G., 2010. Separation of net ecosystem exchange into assimilation and respiration using a light response curve approach: critical issues and global evaluation. Glob. Change Biol. 16 (1), 187–208.

Lavigne, M., Foster, R., Goodine, G., 2004. Seasonal and annual changes in soil respiration in relation to soil temperature, water potential and trenching. Tree Physiol. 24 (4), 415.

Law, B., Kelliher, F., Baldocchi, D., Anthoni, P., Irvine, J., Moore, D., Van Tuyl, S., 2001a. Spatial and temporal variation in respiration in a young ponderosa pine forests during a summer drought. Agric. Forest Meteorol. 110 (1), 27–43.

Law, B., Ryan, M., Anthoni, P., 1999. Seasonal and annual respiration of a ponderosa pine ecosystem. Glob. Change Biol. 5 (2), 169–182.

Law, B., Van Tuyl, S., Cescatti, A., Baldocchi, D., 2001. Estimation of leaf area index in open-canopy ponderosa pine forests at different successional stages and management regimes in Oregon. Agric. Forest Meteorol. 108 (1), 1–14.

Lloyd, J., Taylor, J.A., 1994. On the temperature-dependence of soil respiration. Funct. Ecol. 8 (3), 315–323.

Luo, Y., Gerten, D., Le Maire, G., Parton, W.J., Weng, E., Zhou, X., Keough, C., Beier, C., Ciais, P., Cramer, W., Dukes, J.S., Emmett, B., Hanson, P.J., Knapp, A., Linder, S., Nepstad, D., Rustad, L., 2008. Modeled interactive effects of precipitation, temperature, and $[CO_2]$ on ecosystem carbon and water dynamics in different climatic zones. Glob. Change Biol. 14 (9), 1986–1999.

Martinez-Vilalta, J., Sala, A., Pinol, J., 2004. The hydraulic architecture of pinaceae – a review. Plant Ecol. 171 (1–2), 3–13.

Meinzer, F., 2002. Co-ordination of vapour and liquid phase water transport properties in plants. Plant Cell Environ. 25 (2), 265–274.

Metcalfe, D.B., Meir, P., Aragao, L.E.O.C., Lobo-do Vale, R., Galbraith, D., Fisher, R.A., Chaves, M.M., Maroco, J.P., da Costa, A.C.L., de Almeida, S.S., Braga, A.P., Goncalves, P.H.L., de Athaydes, J., da Costa, M., Portela, T.T.B., de Oliveira, A.A.R., Malhi, Y., Williams, M., 2010. Shifts in plant respiration and carbon use efficiency at a large-scale drought experiment in the eastern amazon. New Phytol. 187 (3), 608–621.

Monteith, J., Unsworth, M., 2007. Principles of Environmental Physics, 2nd ed. Academic Press.

Noormets, A., Gavazzi, M.J., Mcnulty, S.G., Domec, J.-C., Sun, G., King, J.S., Chen, J., 2010. Response of carbon fluxes to drought in a coastal plain loblolly pine forest. Glob. Change Biol. 16 (1), 272–287.

Oren, R., Phillips, N., Katul, G., Ewers, B., Pataki, D., 1998. Scaling xylem sap flux and soil water balance and calculating variance: a method for partitioning water flux in forests. Ann. Sci. Forest. 55 (1–2), 191–216.

Oren, R., Sperry, J., Katul, G., Pataki, D., Ewers, B., Phillips, N., Schafer, K., 1999. Survey and synthesis of intra- and interspecific variation in stomatal sensitivity to vapour pressure deficit. Plant Cell Environ. 22 (December (12)), 1515–1526.

Panek, J., Goldstein, A., 2001. Response of stomatal conductance to drought in ponderosa pine: implications for carbon and ozone uptake. Tree Physiol. 21 (5), 337–344.

Pearcy, R.W., Schulze, E.D., Zimmermann, R., 1989. Measurement of transpiration and leaf conductance. In: Plant Physiological Ecology. Chapman and Hall, London, New York, pp. 137–160.

Pereira, J.S., Mateus, J.A., Aires, L.M., Pita, G., Pio, C., David, J.S., Andrade, V., Banza, J., David, T.S., Paco, T.A., Rodrigues, A., 2007. Net ecosystem carbon exchange in three contrasting Mediterranean ecosystems – the effect of drought. Biogeosciences 4 (5), 791–802.

Phillips, N., Ryan, M., Bond, B., McDowell, N., Hinckley, T., Cermak, J., 2003. Reliance on stored water increases with tree size in three species in the pacific northwest. Tree Physiol. 23 (4), 237–245.

Pierce, J., Meyer, G., Jull, A., 2004. Fire-induced erosion and millennialscale climate change in northern ponderosa pine forests. Nature 432 (7013), 87–90.

Pinheiro, J., Bates, D., DebRoy, S., Sarkar, D., Team, R.D.C., 2010. nlme: Linear and Nonlinear Mixed Effects Models. R Package Version 3.1-97.

R Development Core Team, 2010. R: A Language and Environment for Statistical Computing. R Foundation for Statistical Computing, Vienna, Austria, ISBN 3-900051-07-0.

Reichstein, M., Papale, D., Valentini, R., Aubinet, M., Bernhofer, C., Knohl, A., Laurila, T., Lindroth, A., Moors, E., Pilegaard, K., Seufert, G., 2007. Determinants of terrestrial

ecosystem carbon balance inferred from European eddy covariance flux sites. Geophys. Res. Lett. 34 (1), L01402.
Reichstein, M., Tenhunen, J., Roupsard, O., Ourcival, J., Rambal, S., Miglietta, F., Peressotti, A., Pecchiari, M., Tirone, G., Valentini, R., 2002. Severe drought effects on ecosystem CO_2 and H_2O fluxes at three Mediterranean evergreen sites: revision of current hypotheses? Glob. Change Biol. 8 (10), 999–1017.
Ruehr, N.K., Offermann, C.A., Gessler, A., Winkler, J.B., Ferrio, J.P., Buchmann, N., Barnard, R.L., 2009. Drought effects on allocation of recent carbon: from beech leaves to soil CO_2 efflux. New Phytol. 184 (4), 950–961.
Ryan, M.G., 2011. Tree responses to drought. Tree Physiol. 31 (3), 237–239.
Sardans, J., Penuelas, J., Ogaya, R., 2008. Drought-induced changes in c and n stoichiometry in a quercus ilex mediterranean forest. Forest Sci. 54 (5), 513–522.
Schroter, D., Cramer, W., Leemans, R., Prentice, C., Araujo, M., Arnell, N., Bondeau, A., Bugmann, H., Carter, T., Gracia, C., de la Vega-Leinert, A., Erhard, M., Ewert, F., Glendining, M., House, J., Kankaanpaa, S., Klein, R., Lavorel, S., Lindner, M., Metzger, M., Meyer, J., Mitchell, T., Reginster, I., Rounsevell, M., Sabate, S., Sitch, S., Smith, B., Smith, J., Smith, P., Sykes, M., Thonicke, K., Thuiller, W., Tuck, G., Zaehle, S., Zierl, B., 2005. Ecosystem service supply and vulnerability to global change in Europe. Science 310 (5752), 1333–1337.
Schulze, E., Cermak, J., Matyssek, R., Penka, M., Zimmermann, R., Vasicek, F., Gries, W.w., Kucera, J., 1985. Canopy transpiration and water fluxes in the xylem of the trunk of Larix and Picea trees – a comparison of xylem flow, porometer and cuvette measurements. Oecologia 66 (4), 475–483.
Schwalm, C.R., Williams, C., Schaefer, K., Arneth, A., Bonal, D., Buchmann, N., Chen, J., Law, B.E., Lindroth, A., Luyssaert, S., Reichstein, M., Richardson, A.D., 2009. Assimilation exceeds respiration sensitivity to drought: a FLUXNET synthesis. Glob. Change Biol. 16 (2), 657–670.
Tang, J., Baldocchi, D., Xu, L., 2005. Tree photosynthesis modulates soil respiration on a diurnal time scale. Glob. Change Biol. 11, 1298–1304.
Thomas, C.K., Law, B.E., Irvine, J., Martin, J.G., Pettijohn, J.C., Davis, K.J., 2009. Seasonal hydrology explains interannual and seasonal variation in carbon and water exchange in a semiarid mature ponderosa pine forest in central Oregon. J. Geophys. Res. Biogeosci. 114, G04006, http://dx.doi.org/10.1029/2009JG001010.
Unger, S., Maguas, C., Pereira, J.S., Aires, L.M., David, T.S., Werner, C., 2009. Partitioning carbon fluxes in a Mediterranean oak forest to disentangle changes in ecosystem sink strength during drought. Agric. Forest Meteorol. 149 (6–7), 949–961.
Vickers, D., Thomas, C.K., Pettijohn, C., Martin, J.G., Law, B.E., 2012. Five years of carbon fluxes and inherent water-use efficiency at two semi-arid pine forests with different disturbance histories. Tellus Ser. B: Chem. Phys. Meteorol. 64, 17159.
Williams, M., Law, B., Anthoni, P., Unsworth, M., 2001. Use of a simulation model and ecosystem flux data to examine carbon–water interactions in ponderosa pine. Tree Physiol. 21 (5), 287–298.
Zuur, A., Ieno, E.N., Walker, N.J., Saveliev, A.A., Smith, G.M., 2009. Mixed Effects Models and Extensions in Ecology with R. Springer.